BIOCHEMISTRY
including biophysical chemistry & molecular biology

Rapid Report

pubs.acs.org/biochemistry

Cysteine Substitution and Labeling Provide Insight into Channelrhodopsin-2 Ion Conductance

Ryan Richards and Robert E. Dempski*

Department of Chemistry and Biochemistry, Worcester Polytechnic Institute, Worcester, Massachusetts 01609, United States

Supporting Information

ABSTRACT: Channelrhodopsin-2 is a light-activated cation channel. However, the mechanism of ion conductance is unresolved. Here, we performed cysteine scanning mutagenesis on transmembrane domain 7 followed by labeling with a methanethiosulfonate compound. Analysis of our results shows that residues that line the putative pore and interface with adjacent transmembrane domains 1 and 3, as proposed by our channelrhodopsin-2 homology model, affect ion conductance, decay kinetics, and/or off kinetics. Combined, these results suggest that negative charges at the extracellular side of transmembrane domain 7 funnel cations into the pore.

Channelrhodopsin-2 (ChR2) is a light-activated cation channel endogenous to *Chlamydomonas reinhardtii*. Together with channelrhodopsin-1 (ChR1), activation of ChR2 is the first committed step in phototaxis.[1,2] ChR2 is structurally similar to microbial ion pump rhodopsins with a seven-transmembrane domain motif and the chromophore all-trans retinal bound to a conserved lysine in transmembrane domain 7 (TM7) (for ChR2, K257). ChR2 is one member of a growing subfamily of rhodopsins that function as ion channels and have proton pumping capability.[3] More specifically, ChR2 is an inwardly rectified cation channel that can conduct cations ($H^+ > Li^+ > Na^+ > K^+ > Ca^{2+}$) of multiple valencies with a pore diameter of ~6.4 Å.[2,4] Maximal activation of ChR2 occurs with 470 nm light that isomerizes the retinal moiety around C13. Retinal isomerization begins the proton transfer pathway and conformational movements inducing the opening of the channel. Activation of ChR2 results in an initial transient peak current (I_P), which then decays to a steady state current (I_S) under prolonged light exposure (Figure S1A).

ChR2 is a central tool in the emerging field of optogenetics, in which excitable cells expressing ChR2 can be controlled with light.[5] However, the molecular determinants that contribute to ion permeation remain unresolved. Analysis of electron paramagnetic resonance (EPR) and Fourier transform infrared spectroscopy (FTIR) experiments has greatly improved our understanding of the early stages of pore formation.[6−9] Elucidation of the crystal structure of the ChR variant C1C2, which includes transmembrane (TM) domains 1−5 of ChR1 and TM6 and TM7 of ChR2, has provided a scaffold for investigating the molecular mechanism of ChR2 function.[10] Inspection of this crystal structure shows that the extracellular side of the protein contains a large water-filled electronegative vestibule, which includes TM1−TM3 and TM7. Analysis of cysteine scanning experiments has shown that residues on the extracellular side of TM3 contribute to the cation permeation pathway of ChR2.[11] This vestibule is closed further down the pore by an occlusion site comprised of hydrogen bonds among S63, E90, and N258. A second occlusion site is found at Y70 on the intracellular side. A charged residue on TM2 (E90) is crucial for proper cation flux and likely contributes to cation gating.[7,12] Charge inversion of E90 to lysine turns ChR2 into a Cl^- channel.[13,14]

While inspection of the C1C2 chimera crystal structure has revealed that TM7 forms part of the extracellular electronegative pore, the contribution of TM7 to the permeation pathway of ChR2 is unresolved. Therefore, we performed cysteine scanning mutagenesis and 2-sulfonatoethylmethanethiosulfonate (MTSES) labeling on residues that comprise TM7 preceding K257 to elucidate the role of TM7 in ion permeation. MTSES labeling introduces a negative charge upon site-specific labeling. The ability to site-specifically introduce charge is a powerful tool for identifying the contribution of specific residues to the permeation pathway of ion channels.[15] We compared photocurrents and kinetics between wild-type (wt) ChR2 and constructs that contained single-cysteine replacements within TM7 as ChR2. Photoactivation was performed with a 470 nm light-emitting diode (LED) using two-electrode voltage clamp electrophysiology following heterologous expression in *Xenopus laevis* oocytes (see the Supporting Information for details).

Cysteine replacement of H249, D253, L254, and S256 resulted in ChR2 proteins that had photocurrents of <40 nA. This could be due to nonfunctional protein or protein that did not traffic to the plasma membrane. D253C is required for function as this residue serves as the proton acceptor from the Schiff base during the photocycle.[6] Furthermore, S256 is located directly above the Schiff base in the retinal binding pocket where mutation could alter the absorption maximum, explaining the lack of a photocurrent. Cysteine replacement at position 252 resulted in significantly greater I_P and I_S photocurrents when compared to those of ChR2. In contrast, cysteine replacement at positions V242, Y243, G244, S245, T246, G248, and T250 demonstrated significantly smaller I_P and I_S photocurrents compared to those of wt ChR2 (Figure S1B).

Received: July 1, 2015
Revised: August 30, 2015
Published: August 31, 2015

DOI: 10.1021/acs.biochem.5b00738
Biochemistry 2015, 54, 5665−5668

ChR2 I_P, but not I_S, undergoes rundown upon repeated photostimuli.[2] To quantify whether MTSES labeling altered ChR2 photocurrents, the following protocol was used. First, light was applied to oocytes expressing ChR2 at a membrane potential (V_m) of −120 to 60 mV in 20 mV steps (negative control). Following a wait time of 7 min, a second stimulus at −120 to 60 mV was applied. During the wait time, oocytes were labeled with MTSES in MTS(+) buffer or washed in MTS(−) buffer to serve as a positive control (see the Supporting Information for details). Photocurrents from the second stimulus were normalized to the first stimulus. The normalized unlabeled and labeled photocurrents were then compared as a percent difference to determine the effect of labeling (Figure 1). We used this approach as the recovery of the transient peak response for wt ChR2 was variable between batches of oocytes expressing ChR2.[16]

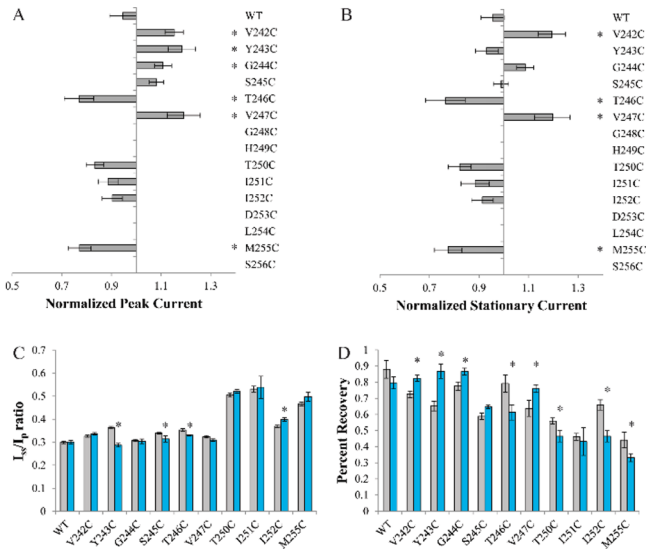

Figure 1. MTSES labeling effects on ChR2 cysteine mutant photocurrents. Normalized (A) I_P and (B) I_S photocurrent responses following labeling of ChR2 mutants. (C) Steady state to peak current ratios and (D) percent recovery of the second photostimulus (see the Supporting Information for details; gray bars, unlabeled control; blue bars, MTSES-labeled; V_m = −120 mV; n = 3−11). *p < 0.05. Error bars indicate the standard error of the mean. Data in panels A and B are displayed as a percentage of the control.

There are nine cysteine residues in ChR2. No functional effect following MTSES labeling for the wt ChR2 was observed. For several functional cysteine mutants, MTSES labeling had no effect on the I_P or I_S amplitude when compared to that of wt ChR2 at a V_m of −120 mV (Figure 1). No functional effect upon MTSES application could be the result of no labeling or no functional effect upon labeling. A significant increase in I_P upon MTSES labeling was observed for V242C, Y243C, G244C, and V247C, while a significant decrease was observed for T246C and M255C. MTSES labeling induced an increase in I_S for V242C and V247C and produced a decrease in I_S for T246C and M255C. It is interesting to note that the closed ChR2 must have a large open extracellular cavity as MTSES reagents can label a residue (M255C) deep within the pore. We also investigated I_s/I_p ratios and percent channel recovery upon MTSES labeling (Figure 1C,D). I_s/I_p ratios represent channel inactivation from the high-conducting O1 state to the low-conducting O2 state during prolonged light exposure, an effect not observed under single-turnover conditions. The largest effect on channel inactivation was seen at Y243C where the I_s/I_p ratio decreased from 0.36 ± 0.05 to 0.30 ± 0.01 upon MTSES labeling. This correlates with an increase in ion conductance for this mutant for only I_p, suggesting an increase in conductance during the early O1 state.

Percent recovery gives insight into the efficiency of ChR2 recovering to the initial dark state. Recovery of MTSES-labeled constructs was higher for V242C, Y243C, G244C, and V247C, while it was lower for T246C, I252C, and M255C compared to that of the unlabeled wait control. Labeling of wt ChR2 had no effect on I_s/I_p or recovery in the dark. Recovery of of ChR2 is dependent on the reisomerization of retinal to the all-trans isomer and the reprotonation of E90, which is deprotonated during the photocycle.[6] Accelerated recovery of ChR2 can be achieved by a low external pH[2]. Labeled cysteine constructs that increased recovery may be facilitated by funneling protons to the extracellular vestibule, increasing the accessibility to E90. We propose the decrease in recovery for T246C, I252C, and M255C is likely caused by changing the electrostatic environment around E90 and the retinal binding pocket.

Photoactivation of ChR2 results in an initial transient peak current that decays rapidly to a steady state current under continuous illumination (Figure S1A). Decay rates were fitted with a monoexponential function. Off rates were fitted with a biexponential function. Under prolonged light exposure, off kinetics are biphasic with a slow and fast component representing multiple decay processes. Decay kinetics are voltage-independent; however, off kinetics are dependent on the holding potential under our experimental conditions (Figure S2). Analysis of changes in the response to photostimulus upon cysteine substitution provides information about channel gating. Cysteine replacement had a significant effect on the decay kinetics (from I_P to I_S) (Table 1). V242C and I252C resulted in accelerated decay kinetics, while G244C, S245C, and T246C had slower decay rates (Table 1). Cysteine replacement had a significant effect on the off kinetics (from I_S to off), resulting in faster rates for V242C and T250C but slower rates for G244C, S245C, T246C, V247C, and I252C. Labeling with MTSES significantly increased τ_{decay} for T250C

Table 1. Effect of Cysteine Replacement or MTSES Labeling on Decay and Off Kinetics of ChR2 Photocurrents[a]

	decay kinetics (ms)		off kinetics (ms)	
	unlabeled control	MTSES-labeled	unlabeled control	MTSES-labeled
wt ChR2	43.1 ± 1.7	45.6 ± 3.1	7.3 ± 0.1	6.7 ± 0.2
V242C	47.8 ± 4.8	40.1 ± 2.7	8.7 ± 0.3[b]	8.5 ± 02
Y243C	33.2 ± 2.5[b]	29.3 ± 1.3	7.4 ± 0.2	7.1 ± 0.3
G244C	35.7 ± 1.1[b]	39.7 ± 2.2	6.6 ± 0.002[b]	6.8 ± 0.002[c]
S245C	24.5 ± 0.9[b]	25.3 ± 1.8	6.2 ± 0.1[b]	5.8 ± 0.1
T246C	29.5 ± 2.2[b]	26.5 ± 0.9	5.7 ± 0.2[b]	5.6 ± 0.1
V247C	40.1 ± 2.2	37.2 ± 1.8	5.7 ± 0.1[b]	6.3 ± 0.1[c]
T250C	40.1 ± 4.6	29.6 ± 3.4[c]	8.6 ± 0.5[b]	8.4 ± 0.3
I251C	34.0 ± 3.1[b]	30.4 ± 1.8	6.2 ± 0.4	7.1 ± 0.4
I252C	67.6 ± 4.0[b]	70.1 ± 3.3	6.2 ± 0.2[b]	6.2 ± 0.1
M255C	37.3 ± 4.0	35.1 ± 2.4	6.6 ± 0.3	6.4 ± 0.1

[a]Current traces were fit to a monoexponential or biexponential function for decay or off kinetics, respectively (V_m = −120 mV; n = 5−11). [b]p < 0.05 for unlabeled control compared to wt. [c]p < 0.05 for MTSES-labeled compared to the unlabeled control. Errors indicate the standard error of the mean.

DOI: 10.1021/acs.biochem.5b00738
Biochemistry 2015, 54, 5665−5668

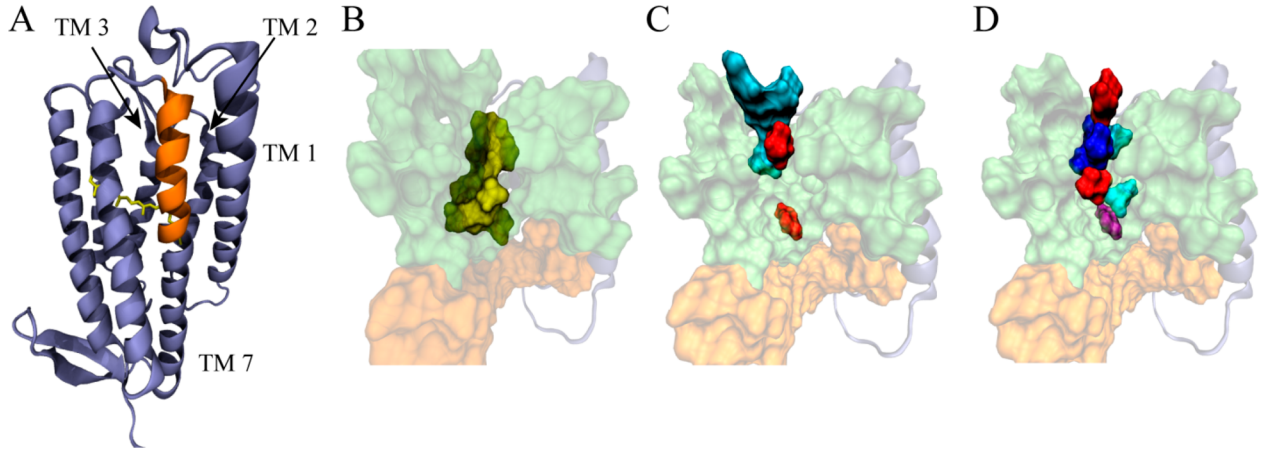

Figure 2. Homology model of ChR2. (A) Equilibrated ChR2 structure with cysteine mutations colored orange and all-trans retinal colored yellow. (B) Location of cysteine mutations that had no effect on ChR2 function upon labeling or were nonfunctional and/or had a low level of expression. (C) Location of residues that upon cysteine mutagenesis affected ion conductance. Mutations that had a significant increase in peak current upon MTSES labeling are colored cyan, while those that had a decrease are colored red. (D) Location of residues that altered ChR2 kinetics upon cysteine replacement. Single-cysteine mutants that affected decay kinetics only (purple), off kinetics only (red), or both (cyan) when compared to wt are shown. Residues that had a significant effect on kinetics upon labeling with MTSES are colored blue. Images were created using Visual Molecular Dynamics Software.[20]

from 40.1 ± 4.6 to 29.6 ± 3.4 ms (n = 4). This result suggests that the transition from O1 to O2 is accelerated in the presence of a negative charge or steric bulk at this position. In contrast, τ_{off} was slower upon MTSES labeling for G244C and V247C (Table 1). Similar to those for decay kinetics, these results suggest that channel gating is impaired in the presence of a negative charge or steric hindrance at these positions.

To spatially inspect the results of our experiments, we developed an equilibrated model of ChR2 based on the crystal structure of the channelrhodopsin chimera C1C2 (Figure S3).[10] The ChR2 sequence was built on C1C2 using the SWISS-MODEL database following a sequence alignment (see the Supporting Information for details).[17−20] When compared to C1C2, ChR2 is 76.3% identical and 91.7% similar using the Waterman−Eggert scoring system (Figure S4).[21] Within the context of our homology model, residues that affected I_s and I_p were located at the interface of TM7 and TM1, with the exception of M255, which is oriented into the lipid bilayer (Figure 2).

This indicates that even in the closed state, ChR2 is sufficiently flexible so that residues adjacent to another TM domain can be labeled. V242 and T246 are in proximity of R115 and Q117, which upon cysteine replacement and MTS labeling affect ion conductance and permeability.[11] Introducing a longer-chain negative charge at these positions may facilitate interhelical hydrogen bonding that enhances or reduces ion conductance for V242C or T246C, respectively. Placing a negative charge at the top of the vestibule, as with labeling of V242C, Y243C, G244C, and V247C, may serve to increase the access of the cation to the pore, which results in an increase in I_p ion conductance.[22] Curiously, M255C had a detrimental effect on I_p and I_s, when labeled, but faces into the membrane. Previously, it was shown that mutation of M255 to a polar residue (M255S) results in highly reduced photocurrents.[4] However, free cysteines behave like hydrophobic residues, which is evident by the modest photocurrents of M255C.[23] This suggests that introduction of a negative charge with MTSES at this position disturbs the interaction between the membrane and TM7, resulting in severely reduced conductance.

Analysis of our experimental results also indicates that the extracellular side of TM7 forms, in part, the permeation pathway for ChR2. Residues that are located near the extracellular interface had the largest effect on ion conductance, while those closer to the first occlusion site had no observable effect or were not accessible for labeling, with the exception of M255C. Compared to other opsin pumps, the backbone of ChR2 undergoes large conformational changes preceding conductance.[24] This flexibility likely contributes to the accessibility of residues for labeling. We also observed that most cysteine mutations in TM7 altered one or both kinetic parameters. Furthermore, only T246C, V247C, and I251C resulted in a significant difference in kinetics when compared to those of the control. Mutations that resulted in little to no photocurrent (D253, H249, and S256) have a high degree of sequence homology among algal rhodopsins.

As most of TM7 has little to no conservation, we postulate that the diversity among residues in TM7 may contribute to the unique functionality and broad selectivity of ChR2 compared to other rhodopsins. Moreover, labeling of cysteine constructs in the extracellular vestibule with a negative charge likely causes a funneling effect to increase the access of the cation to the permeation pathway.

■ ASSOCIATED CONTENT

Supporting Information

The Supporting Information is available free of charge on the ACS Publications website at DOI: 10.1021/acs.biochem.5b00738.

Supplemental figures and experimental procedures (PDF)

■ AUTHOR INFORMATION

Corresponding Author

*E-mail: rdempski@wpi.edu.

Author Contributions

The manuscript was written by both authors.

DOI: 10.1021/acs.biochem.5b00738
Biochemistry 2015, 54, 5665−5668

Funding

The work was supported by WPI and the Extreme Science and Engineering Discovery Environment (XSEDE) and by National Science Foundation Grant MCB140113.

Notes

The authors declare no competing financial interest.

REFERENCES

(1) Sineshchekov, O. A., Jung, K. H., and Spudich, J. L. (2002) Two rhodopsins mediate phototaxis to low- and high-intensity light in Chlamydomonas reinhardtii. *Proc. Natl. Acad. Sci. U. S. A. 99*, 8689−8694.

(2) Nagel, G., Szellas, T., Huhn, W., Kateriya, S., Adeishvili, N., Berthold, P., Ollig, D., Hegemann, P., and Bamberg, E. (2003) Channelrhodopsin-2, a directly light-gated cation-selective membrane channel. *Proc. Natl. Acad. Sci. U. S. A. 100*, 13940−13945.

(3) Klapoetke, N. C., Murata, Y., Kim, S. S., Pulver, S. R., Birdsey-Benson, A., Cho, Y. K., Morimoto, T. K., Chuong, A. S., Carpenter, E. J., Tian, Z., Wang, J., Xie, Y., Yan, Z., Zhang, Y., Chow, B. Y., Surek, B., Melkonian, M., Jayaraman, V., Constantine-Paton, M., Wong, G. K.-S., and Boyden, E. S. (2014) Independent optical excitation of distinct neural populations. *Nat. Methods 11*, 338−346.

(4) Richards, R., and Dempski, R. E. (2012) Re-introduction of transmembrane serine residues reduce the minimum pore diameter of channelrhodopsin-2. *PLoS One 7*, e50018.

(5) Boyden, E. S., Zhang, F., Bamberg, E., Nagel, G., and Deisseroth, K. (2005) Millisecond-timescale, genetically targeted optical control of neural activity. *Nat. Neurosci. 8*, 1263−1268.

(6) Lórenz-Fonfría, V. A., Resler, T., Krause, N., Nack, M., Gossing, M., Fischer von Mollard, G., Bamann, C., Bamberg, E., Schlesinger, R., and Heberle, J. (2013) Transient protonation changes in channelrhodopsin-2 and their relevance to channel gating. *Proc. Natl. Acad. Sci. U. S. A. 110*, E1273−E1281.

(7) Kuhne, J., Eisenhauer, K., Ritter, E., Hegemann, P., Gerwert, K., and Bartl, F. (2015) Early formation of the ion-conducting pore in channelrhodopsin-2. *Angew. Chem., Int. Ed. 54*, 4953−4957.

(8) Sattig, T., Rickert, C., Bamberg, E., Steinhoff, H. J., and Bamann, C. (2013) Light-induced movement of the transmembrane HelixB in channelrhodopsin-2. *Angew. Chem., Int. Ed. 52*, 9705−9708.

(9) Krause, N., Engelhard, C., Heberle, J., Schlesinger, R., and Bittl, R. (2013) Structural differences between the closed and open states of channelrhodopsin-2 as observed by EPR spectroscopy. *FEBS Lett. 587*, 3309−3313.

(10) Kato, H. E., Zhang, F., Yizhar, O., Ramakrishnan, C., Nishizawa, T., Hirata, K., Ito, J., Aita, Y., Tsukazaki, T., Hayashi, S., Hegemann, P., Maturana, A. D., Ishitani, R., Deisseroth, K., and Nureki, O. (2012) Crystal structure of the channelrhodopsin light-gated cation channel. *Nature 482*, 369−374.

(11) Gaiko, O., and Dempski, R. E. (2013) Transmembrane domain three contributes to the ion conductance pathway of channelrhodopsin-2. *Biophys. J. 104*, 1230−1237.

(12) Ruffert, K., Himmel, B., Lall, D., Bamann, C., Bamberg, E., Betz, H., and Eulenburg, V. (2011) Glutamate residue 90 in the predicted transmembrane domain 2 is crucial for cation flux through channelrhodopsin 2. *Biochem. Biophys. Res. Commun. 410*, 737−743.

(13) Wietek, J., Wiegert, J. S., Adeishvili, N., Schneider, F., Watanabe, H., Tsunoda, S. P., Vogt, A., Elstner, M., Oertner, T. G., and Hegemann, P. (2014) Conversion of channelrhodopsin into a light-gated chloride channel. *Science 344*, 409−412.

(14) Berndt, A., Lee, S. Y., Ramakrishnan, C., and Deisseroth, K. (2014) Structure-guided transformation of channelrhodopsin into a light-activated chloride channel. *Science 344*, 420−424.

(15) Akabas, M. H., Stauffer, D. A., Xu, M., and Karlin, A. (1992) Acetylcholine-receptor channel structure probed in cysteine-substitution mutants. *Science 258*, 307−310.

(16) Roberts, J. A., and Evans, R. J. (2007) Cysteine substitution mutants give structural insight and identify ATP binding and activation sites at P2X receptors. *J. Neurosci. 27*, 4072−4082.

(17) Kiefer, F., Arnold, K., Kunzli, M., Bordoli, L., and Schwede, T. (2009) The SWISS-MODEL Repository and associated resources. *Nucleic Acids Res. 37*, D387−392.

(18) Arnold, K., Bordoli, L., Kopp, J., and Schwede, T. (2006) The SWISS-MODEL workspace: a web-based environment for protein structure homology modelling. *Bioinformatics 22*, 195−201.

(19) Peitsch, M. C. (1995) Protein modeling by email. *Bio/Technology 13*, 658−660.

(20) Humphrey, W., Dalke, A., and Schulten, K. (1996) VMD: Visual molecular dynamics. *J. Mol. Graphics 14*, 33−38.

(21) Huang, X. Q., and Miller, W. (1991) A Time-Efficient, Linear-Space Local Similarity Algorithm. *Adv. Appl. Math 12*, 337−357.

(22) Green, W. N., and Andersen, O. S. (1991) Surface-charges and ion channel function. *Annu. Rev. Physiol. 53*, 341−359.

(23) Nagano, N., Ota, M., and Nishikawa, K. (1999) Strong hydrophobic nature of cysteine residues in proteins. *FEBS Lett. 458*, 69−71.

(24) Radu, I., Bamann, C., Nack, M., Nagel, G., Bamberg, E., and Heberle, J. (2009) Conformational changes of channelrhodopsin-2. *J. Am. Chem. Soc. 131*, 7313−7319.

DOI: 10.1021/acs.biochem.5b00738
Biochemistry 2015, 54, 5665−5668